Published in final edited form as:
Angew Chem Int Ed Engl. 2012 January 16; 51(3): 647–651. doi:10.1002/anie.201104147.

Characterization of the Reaction Path and Transition States for RNA Transphosphorylation Models from Theory and Experiment**

Kin-Yiu Wong[*],
BioMaPS Institute for Quantitative Biology Department of Chemistry and Chemical Biology Rutgers, The State University of New Jersey 610 Taylor Road, Piscataway, NJ 08854 (USA)

Hong Gu,
RNA Center and Department of Biochemistry Case Western Reserve University School of Medicine Cleveland, OH 44118 (USA)

Shuming Zhang,
RNA Center and Department of Biochemistry Case Western Reserve University School of Medicine Cleveland, OH 44118 (USA)

Joseph A. Piccirilli[*],
Departments of Biochemistry and Molecular Biology, and Chemistry University of Chicago Chicago, Illinois 60637 (USA)

Michael E. Harris[*], and
RNA Center and Department of Biochemistry Case Western Reserve University School of Medicine Cleveland, OH 44118 (USA)

Darrin M. York[*]
BioMaPS Institute for Quantitative Biology Department of Chemistry and Chemical Biology Rutgers, The State University of New Jersey 610 Taylor Road, Piscataway, NJ 08854 (USA)

Keywords

RNA; transphosphorylation; mechanism; kinetic isotope effects; *ab initio* QM/MM; Feynman's path integral; Kleinert's variational perturbation theory

The elucidation of the chemical mechanisms whereby biological molecules control, regulate and catalyze phosphoryl transfer reactions has profound implications for processes such as transcription, energy storage and transfer, cell signalling and gene regulation.[1, 2] The catalytic properties of RNA, in particular, have application in the design of new biotechnology and implications into the evolutionary origins of life itself.[3] Of primary importance to the understanding of mechanism is the characterization of the transition state for these reactions. Kinetic isotope effects (KIEs) offer one of the most powerful and sensitive experimental probes to interrogate the chemical environment of the transition

**The authors are grateful for financial support from the National Institutes of Health (GM084149 to D.M.Y., R21GM079647 to M.E.H. and AI081987 to J.A.P.). Computational resources were provided by the Minnesota Supercomputing Institute (MSI) and by the NSF TeraGrid through the Texas Advanced Computing Center and National Institute for Computational Sciences under grant number TG-CHE100072.

[*]wongky@biomaps.rutgers.edu; kiniu@alumni.cuhk.netyork@biomaps.rutgers.edumichael.e.harris@case.edujpicciri@uchicago.edu.

Supporting information for this article (Experimental Section; Computational Section; Bond distances and bond orders of transition states; PCM radii and structures) is available on the WWW under http://www.angewandte.org or from the authors.

state.[4-6] However, for complex reactions, theoretical methods are required to interpret the experimental measurements in terms of a detailed mechanistic model that traces the pathway from the reactant state through the transition state and into the product state.[7, 8]

This paper presents experimental and computational results to characterize the mechanism of model phosphoryl transfer reactions that mimic RNA cleavage transesterification catalyzed by enzymes such as RNase A[1] as well as endonucleolytic ribozymes such as the hammerhead, hairpin, hepatitis delta virus (HDV), VS and *glmS* ribozymes.[9-11] Herein, secondary kinetic isotope effects are reported for the cleavage transesterification of a dinucleotide system, which, together with previously reported primary isotope effect measurements,[12, 13] represent a comprehensive characterization of isotope effects for a native (unmodified) RNA system.

Scheme 1 illustrates the general mechanism for the reverse dianionic in-line methanolysis of ethylene phosphate, a model for base-catalysed RNA phosphate transesterification, with phosphoryl oxygen positions labelled in accord with their RNA counterparts. In this study, the free energy profiles for Scheme 1 were determined with density-functional quantum mechanical/molecular mechanical (QM/MM) simulations in explicit solvent.[14-17] These simulations are state-of-the-art, and take into account the dynamical fluctuations of the solute and solvent degrees of freedom in determination of the free energy profiles. In addition, adiabatic reaction energy profiles were determined with solvation effects treated implicitly with a polarizable continuum model (PCM)[18] specifically calibrated for the native and 3′ and 5′ thio-substituted compounds (Figure 1). The 3′ and 5′ thio-substituted compounds model the corresponding chemically modified RNAs that serve as valuable experimental probes of phosphoryl transfer mechanisms catalyzed by ribozymes.[19] The S5′ substitution, for example, in the HDV ribozyme serves as an enhanced leaving group that suppresses the deleterious effect of mutation of a critical cytosine residue, which has been interpreted to support its role as a general acid catalyst.[20] The energy values for stationary points of the native and thio-substituted reactions are in Table 1. Using our recently developed *ab initio* path-integral method based on Kleinert's variational perturbation theory,[7, 21-23] we also calculated kinetic isotope effects, which are shown along with the most relevant experimental values for comparison in Table 2. The agreement that is achieved between the theoretical and experimental results allows a detailed mechanistic interpretation based on the theoretical models.[7, 8]

All of the profiles calculated in this work correspond to associative (or concerted) mechanisms characterized by initial nucleophilic attack, as is typical of phosphate diesters.[6] The departure of the leaving group can be concerted with nucleophilic attack (as in the S5′ substituted reaction) or can occur in a stepwise fashion resulting in the formation of a stable pentavalent phosphorane intermediate. In the stepwise mechanism, two transition states occur: one in which nucleophilic attack occurs (TS_1) and another one in which leaving group departure takes place (TS_2) as indicated in Scheme 1. These transition states themselves can be characterized as either "early" or "late", depending on the degree of P-O2′ and P-O5′ bond formation/cleavage.

Native reaction: the late transition state is rate-controlling

The density-functional QM/MM free energy profile[24, 25] and PCM adiabatic reaction profile for the native reaction are very similar (Fig. 1, top). Both profiles describe an associative mechanism, and exhibit distinct TS_1 and TS_2 transition states separated by a shallow, metastable intermediate, with TS_2 rate controlling. Comparison of the activation free energy values from the QM/MM simulations and adiabatic reaction profiles (including zero-point and thermal corrections, Table 1 bottom) indicate that the TS_1 are very similar in

activation energy (18.8 and 18.6 kcal/mol, respectively), whereas the TS_2 is 3.1 kcal/mol higher in the QM/MM simulation. The rate-controlling TS_2 itself has considerable "late" character in which cleavage of the exocyclic P-O5′ bond is advanced (Δbond in Table 1). This result derives from a combination of ring strain effects and differential solvation of the cyclic versus acyclic phosphates.[8, 29] The calculated density-functional free energy barrier with PCM solvation (21.0 kcal/mol) is in close agreement with that estimated from the experimental rate for UpG transphosphorylation extrapolating to the infinite pH limit in the rate expression (i.e., assuming the nucleophile is always in deprotonated form) and assuming unit transmission coefficient (19.9 kcal/mol).[12] This result, taken together with the consistency between the PCM reaction profile and the profile derived from the QM/MM simulations with explicit solvent (Fig. 1, top), suggests that the density-functional PCM calculations sufficiently capture the essential features of the solvation effects on the profile to determine kinetic isotpe effects. The close agreement between the calculated and experimental KIEs (shown below) further supports this supposition.

The primary KIE values calculated using our *ab initio* path-integral method[7, 21-23] are listed in Table 2, and are in good agreement with experimental results. Here, by "good agreement", we refer to agreement within the resolution of the kinetic isotope effects as being large inverse (less than 0.97), inverse (0.97-0.99), near unity (0.99-1.01), normal (1.01-1.03) and large normal (greater than 1.03). In the experiment, the model reaction for the RNA transesterification is the base-catalyzed 2′-O-transphosphorylation of the RNA dinucleotide 5′-UpG-3′.[12] Since both 2′OH deprotonation and 2′O-P bond formation will contribute to the observed KIE, the values reported here for $^{18}k_{Nu}$ and $^{18}k_{Lg}$ (at the infinite pH limit) do not include the equilibrium isotope effect on alcohol deprotonation. The inverse value of $^{18}k_{Nu}$ (0.981) and the large normal value of $^{18}k_{Lg}$ (1.034) measured by experiment[12] agree well with the values calculated in the present work (0.968 and 1.059 in Table 2). In contrast to the rate-controlling TS_2 transition state, our calculated value of $^{18}k_{Nu}$ based on the TS_1 transition state is normal (1.017), and $^{18}k_{Lg}$ is close to unity (1.006). This lends credence to the interpretation that the measured KIE values for the native (UpG transphosphorylation) reaction are consistent with a rate-controlling transition state that is characterized by an almost fully formed P-O2′ bond and an almost fully cleaved P-O5′ bond (Table 1 and Fig 2).

The anharmonic contributions to all primary KIE calculations estimated by our *ab initio* path-integral method are small in the present work (though anharmonicity has been shown to be large for some other reactions[7]). The largest anharmonic contribution is only about 0.3%. Hence, in this study, we computed the anharmonic contributions in the KIE only for the primary isotopomers (i.e., the X2′ and X5′ atoms) listed in Table 2.

S3′ reaction: the measured KIE values correspond to an early transition state

In comparison with the native reaction, the thio effects on the 3′ position lead to a reaction profile characterized by two transition states separated by a kinetically distinct intermediate (Figure 1 bottom and Table 1). The calculated barriers of the two transition states are quite similar to one another (less than 1 kcal/mol difference), and both are lower than the rate-controlling transition state of the native reaction by 3 kcal/mol or more. This result indicates that the 3′ thio-substituted reaction rate should be faster than the native reaction, which is consistent with experimental measurements for 3′ thio-substituted dinucleotides.[13, 30, 31] The lower barrier arises from a combination of stabilizing electronic effects of the soft sulfur in the equatorial position of the pentavalent transition state that is able to help delocalize charge, and partial alleviation of ring strain due the longer P-S3′ bond. Solvation effects are

also present, but are less pronounced than at the non-bridge positions that carry a formal negative charge.

Despite the similarity in their barrier heights, the TS_1 and TS_2 for the S3′ reaction produce significantly different primary KIE signatures. The calculated TS_1 displays large normal and close to unity primary KIE values for the nucleophile ($^{18}k_{Nu}$) and leaving group ($^{18}k_{Lg}$), respectively, whereas the calculated TS_2 exhibits near unity and large normal primary KIE values, respectively (Table 2). The experimental KIE values for the reaction with a *m*-nitrobenzyl leaving group (pK_a=14.9)[32-34] exhibits an anomalously large normal ($^{18}k_{Nu}$ =1.119) and moderate normal ($^{18}k_{Lg}$ =1.011) nucleophile and leaving group KIEs[13], respectively, consistent with the signature of the TS_1 transition state (Table 1 and Fig 2). This experimental $^{18}k_{Nu}$ value[13] reflects a reaction from the ground state in which the 2′O is *not* deprotonated and includes a somewhat large normal contribution of 2-4% due to the equilibrium isotope effect on alcohol deprotonation. Accordingly, the calculated KIE values include this contribution. As in the case for the native reaction, the calculated secondary KIE values of O1P and O2P oxygens for the S3′ reaction are close to unity (Table 2).

S5′ reaction: the unimodal barrier is corresponding to the early transition state

The sulfur-substitution on the 5′ position results in a reaction profile that is unimodal, and lower in activation energy than the native and S3′ reaction profiles (Figure 1 bottom and Table 1). Although sulfur is less apicophilic than oxygen in pentavalent phosphorus compounds,[35] this effect is not predicted to be large in the present calculations, as suggested by the free energy of formation of the TS_1 in the S5′ reaction that is only 2 kcal/mol lower than for the native reaction. The main contribution to the differences in the native and S5′ reaction profiles derives from the nature of the thiolate as an enhanced leaving group relative to the methoxide anion (the pK_a of primary alcohols being typically ~5 pK_a units higher than the corresponding thiols). This leads to the elimination of the TS_2 transition state in the profile, and a shift toward early transition state character (smaller P-O2′ bond order). The value of Δbond in Table 1 and Fig 2 for the transition state is -0.02 Å, but this value reflects the longer bond distance of P—S5′ relative to P— O5′ distances by about 0.5 Å. The rate-controlling barrier for the S5′ reaction is approximately 16.6 kcal/mol, which is the smallest of the reaction models studied here, suggesting this substitution will have the fastest rate. This result is consistent with experimental studies of 5′ substituted reaction models.[13, 36, 37]

The predicted primary KIE values of both $^{18}k_{Nu}$ (1.040) and $^{18}k_{Lg}$ (1.002) for the S5′ model reaction (Table 2) are normal and are in good accord with the experimental results ($^{18}k_{Nu}$: 1.025; $^{18}k_{Lg}$: 1.001) for the cyclization of *m*-nitrobenzyl ribonucleoside phosphodiester with S5′ substitution.[13] This lends support to the notion that the rate-controlling transition state for the S5′ reaction is the TS_1.

Secondary KIEs at the non-bridge phosphoryl oxygen positions

In this work, KIEs were measured for the non-bridge phosphoryl oxygen positions for the native UpG dinucleotide reaction (Table 2). In the present model systems, we have an associative reaction involving a dianionic phosphate diester with the added complexity of coupling between the ring vibrational modes in formation of the transition state. Our measured KIE values of the non-bridge phosphoryl oxygen positions were very close to unity (0.999), and within error are in good agreement with the calculated values of 1.003-1.005 for the native reaction (Table 2). Unlike the calculated differences between the

primary KIE values for the native, S3′ and S5′ reactions, the calculated secondary KIEs are all close to unity.

Conclusion

We report results of density-functional combined QM/MM simulations and solvated adiabatic reaction profiles for native and thio-substituted RNA transphosphorylation reaction models. Kinetic isotope effects were calculated using our recently-developed *ab initio* path-integral method[7, 21-23] that takes into account treatment of internuclear quantum effects. Additionally, we report new measurements of secondary kinetic isotope effects for the native reaction of UpG, the dinucleotide sequence representing the cleavage site in the HDV ribozyme,[9, 12] and make predictions of the secondary isotope effects for thio-substituted reactions. Our results provide an atomic-level picture of the reactions, including a detailed characterization of the rate-controlling transition states that are in agreement with experimental measurements of both the rates and the primary and secondary KIEs. The native reaction is characterized by a rate-controlling transition state corresponding to exocyclic bond cleavage of the leaving group with an inverse primary nucleophile KIE. The S3′ reaction is characterized by two distinct transition states, with the transition state corresponding to nucleophilic attack rather than leaving group departure giving rise to the observed large primary nucleophile KIE value. The S5′ reaction is concerted, and has a unimodal reaction profile with the lowest barrier, and large normal primary KIE values. Unlike the striking differences in the calculated primary KIE values between native and thio-substituted reaction models, all secondary KIE values are close to unity. Together, these results paint a detailed picture of the reaction mechanisms of model phosphoryl transfer reactions.

Supplementary Material

Refer to Web version on PubMed Central for supplementary material.

References

[1]. Perreault DM, Anslyn EV. Angew. Chem., Int. Ed. Engl. 1997; 36:433.

[2]. Westheimer FH. Science. 1987; 235:1173. [PubMed: 2434996]

[3]. Strobel SA, Cochrane JC. Curr. Opin. Chem. Biol. 2007; 11:636. [PubMed: 17981494]

[4]. Strassner T. Angew. Chem. Int. Ed. 2006; 45:6420.

[5]. Kohen, A.; Limbach, H-H. Isotope effects in chemistry and biology. Taylor & Francis; Boca Raton: 2006.

[6]. Hengge AC. Acc. Chem. Res. 2002; 35:105. [PubMed: 11851388]

[7]. Wong K-Y, Richard JP, Gao J. J. Am. Chem. Soc. 2009; 131:13963. [PubMed: 19754046]

[8]. Liu Y, Gregersen BA, Hengge A, York DM. Biochemistry. 2006; 45:10043. [PubMed: 16906762]

[9]. Ferré-D'Amaré AR, Scott WG. Cold Spring Harbor Perspect. Biol. 2010; 2:a003574.

[10]. Scott WG. Curr. Opin. Struct. Biol. 2007; 17:280. [PubMed: 17572081]

[11]. Wong K-Y, Lee T-S, York DM. J. Chem. Theory Comput. 2011; 7:1. [PubMed: 21379373]

[12]. Harris ME, Dai Q, Gu H, Kellerman DL, Piccirilli JA, Anderson VE. J. Am. Chem. Soc. 2010; 132:11613. [PubMed: 20669950]

[13]. Iyer S, Hengge AC. J. Org. Chem. 2008; 73:4819. [PubMed: 18533704]

[14]. Senn HM, Thiel W. Angew. Chem. Int. Ed. 2009; 48:1198.

[15]. van Gunsteren WF, Bakowies D, Baron R, Chandrasekhar I, Christen M, Daura X, Gee P, Geerke DP, Glattli A, Hunenberger PH, Kastenholz MA, Oostenbrink C, Schenk M, Trzesniak D, van d. V. N. F. A. Yu HB. Angew. Chem. Int. Ed. 2006; 45:4064.

[16]. Cao Z, Mo Y, Thiel W. Angew. Chem. Int. Ed. 2007; 46:6811.

[17]. Claeyssens F, Harvey JN, Manby FR, Mata RA, Mulholland AJ, Ranaghan KE, Schutz M, Thiel S, Thiel W, Werner H-J. Angew. Chem. Int. Ed. 2006; 45:6856.

[18]. Cossi M, Scalmani G, Rega N, Barone V. J. Chem. Phys. 2002; 117:43.

[19]. Gaynor JW, Cosstick R. Curr. Org. Chem. 2008; 12:291.

[20]. Das SR, Piccirilli JA. Nat Chem Biol. 2005; 1:45. [PubMed: 16407993]

[21]. Kleinert, H. Path integrals in quantum mechanics, statistics, polymer physics, and financial markets. 3rd ed. World Scientific; Singapore ; River Edge, NJ: 2004.

[22]. Wong K-Y, Gao J. J. Chem. Phys. 2007; 127:211103. [PubMed: 18067342]

[23]. Wong K-Y, Gao J. J. Chem. Theory Comput. 2008; 4:1409. [PubMed: 19749977]

[24]. Brooks BR, Brooks CL III, Mackerell AD Jr. Nilsson L, Petrella RJ, Roux B, Won Y, Archontis G, Bartels C, Boresch S, Caflisch A, Caves L, Cui Q, Dinner AR, Feig M, Fischer S, Gao J, Hodoscek M, Im W, Kuczera K, Lazaridis T, Ma J, Ovchinnikov V, Paci E, Pastor RW, Post CB, Pu JZ, Schaefer M, Tidor B, Venable RM, Woodcock HL, Wu X, Yang W, York DM, Karplus M. J. Comput. Chem. 2009; 30:1545. [PubMed: 19444816]

[25]. Shao Y, Molnar LF, Jung Y, Kussmann J, Ochsenfeld C, Brown ST, Gilbert ATB, Slipchenko LV, Levchenko SV, O'Neill DP, DiStasio RA Jr. Lochan RC, Wang T, Beran GJO, Besley NA, Herbert JM, Lin CY, Van Voorhis T, Chien SH, Sodt A, Steele RP, Rassolov VA, Maslen PE, Korambath PP, Adamson RD, Austin B, Baker J, Byrd EFC, Dachsel H, Doerksen RJ, Dreuw A, Dunietz BD, Dutoi AD, Furlani TR, Gwaltney SR, Heyden A, Hirata S, Hsu C-P, Kedziora G, Khalliulin RZ, Klunzinger P, Lee AM, Lee MS, Liang W, Lotan I, Nair N, Peters B, Proynov EI, Pieniazek PA, Rhee YM, Ritchie J, Rosta E, Sherrill CD, Simmonett AC, Subotnik JE, Woodcock HL III, Zhang W, Bell AT, Chakraborty AK, Chipman DM, Keil FJ, Warshel A, Hehre WJ, Schaefer HF III, Kong J, Krylov AI, Gill PMW, Head-Gordon M. Physical Chemistry Chemical Physics. 2006; 8:3172. [PubMed: 16902710]

[26]. McQuarrie, DA. Statistical mechanics. University Science Books; Sausalito, Calif.: 2000.

[27]. Schaad LJ, Bytautas L, Houk KN. Can. J. Chem. 1999; 77:875.

[28]. Wolfsberg, M. Isotope Effects in Chemistry and Biology. Kohen, A.; Limbach, H-H., editors. Taylor & Francis; Boca Raton: 2006. p. 89

[29]. Liu Y, Gregersen BA, Lopez X, York DM. J. Phys. Chem. B. 2005; 109:19987. [PubMed: 16853584]

[30]. Liu X, Reese CB. Tetrahedron Lett. 1996; 37:925.

[31]. Liu X, Reese CB. J. Chem. Soc. Perkin. Trans. 1. 2000:2227.

[32]. Hengge AC, Onyido I. Curr. Org. Chem. 2005; 9:61.

[33]. Anderson MA, Shim H, Raushel FM, Cleland WW. J. Am. Chem. Soc. 2001; 123:9246. [PubMed: 11562204]

[34]. Sowa GA, Hengge AC, Cleland WW. J. Am. Chem. Soc. 1997; 119:2319.

[35]. López CS, Faza ON, de Lera AR, York DM. Chem. Eur. J. 2005; 11:2081. [PubMed: 15714539]

[36]. Liu X, Reese CB. Tetrahedron Lett. 1995; 36:3413.

[37]. Thomson JB, Patel BK, Jimenez V, Eckart K, Eckstein F. J. Org. Chem. 1996; 61:6273. [PubMed: 11667467]

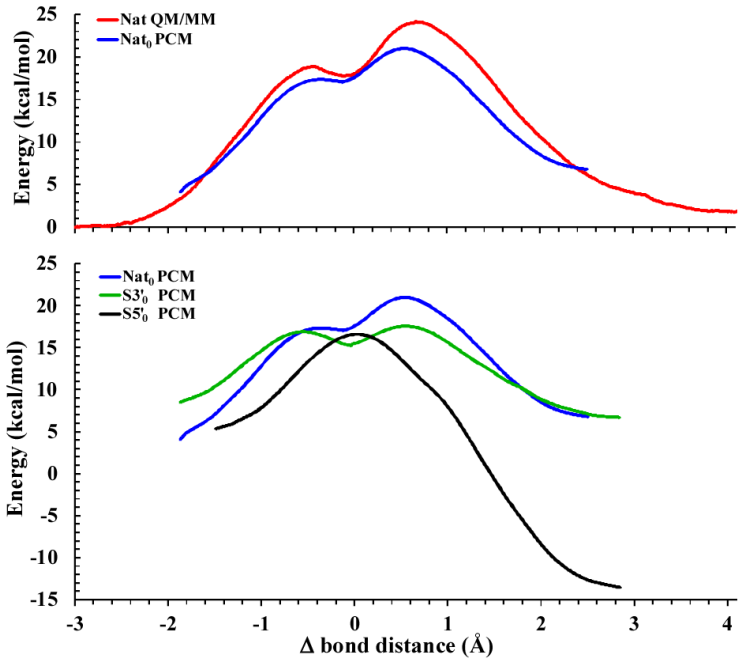

Figure 1.

(Color online) Comparison of density-functional QM/MM free-energy and adiabatic PCM profiles for the native reaction (top), and density-functional adiabatic PCM profiles for native and thio-substituted reactions (bottom) as a function of the difference of the bond distance (Δbond distance) between the breaking bond P—X5′ (X = O for native and S3′, and X = S for S5′ reactions) and the forming bond P—O2′. The adiabatic PCM profiles are mapped from the intrinsic reaction coordinate paths and have been shifted to match the respective rate-controlling free-energy barriers calculated in the decoupled rigid-rotor harmonic-oscillator approximation[26] at 37°C. However, aside from this shift, the adiabatic PCM profiles otherwise do not include zero-point energy or thermal corrections to the free energy, unlike the numbers listed in Table 1 at the bottom.

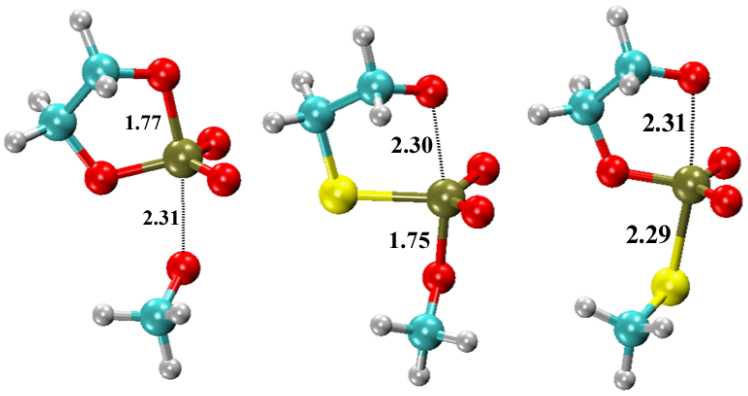

Figure 2.
(Color online) Rate-controlling transition state structures (Scheme 1) consistent with experimental KIE values. Left: Native; Middle: S3′; Right: S5′. The bond distance values are in units of Å.

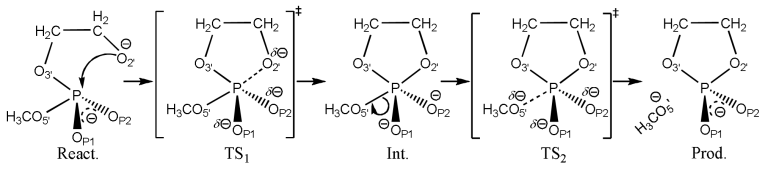

Scheme 1.

General reaction scheme for the (associative) **reverse** of dianionic in-line methanolysis of ethylene phosphate: a model for RNA phosphate transesterification under alkaline conditions. In the present work, the native reaction shown in the scheme is studied as well as reactions that incorporate single thio substitutions in the bridging 3′ (denoted S3′) and leaving group 5′ (denoted S5′) positions. Note: as revealed by the computational analysis herein, not all of the states shown in the scheme exist for every reaction (see text for details).

Table 1

Relative free energy (kcal/mol) and reaction coordinate (Δbond) values (Å) computed for stationary points along the coordinate of the native and thio-substituted RNA phosphate transesterification reaction models shown in Scheme 1.[a]

Reaction	TS_1		Int.		TS_2	
	$\Delta G^{\ddagger}$	Δbond	ΔG	Δbond	$\Delta G^{\ddagger}$	Δbond
Nat QM/MM	18.8[b]	−0.43	17.7[b]	−0.12	**24.1**[b,c]	0.67
Nat_0 PCM	17.3	−0.36	17.0	−0.12	**21.0**[b,c]	0.54
Nat PCM	18.6	−0.36	18.3	−0.12	**21.0**[b]	0.54
S3′ PCM	**16.9**	−0.55	16.0	−0.04	17.8	0.54
S5′ PCM	**16.6**	−0.02	n.a.[d]	n.a.[d]	n.a.[d]	n.a.[d]

[a] Δbond (Å) is defined as the difference of the bond distance between the breaking bond P—X5′ and the forming bond P—O2′. ΔG values are in kcal/mol. Nat_0 is PCM energy (Fig. 1) shifted by the thermal corrections at TS_2. **Boldface** type indicates the rate controlling transition state suggested by comparison with experimental KIE measurements.

[b] Statistical uncertainties are 1.1, 0.8, 1.4 kcal/mol for TS_1, Int., TS_2, respectively.

[c] Experimental estimated barrier for UpG transphosphorylation is 19.9 kcal/mol.[12]

[d] Not applicable as Int. and TS_2 cannot be found.

Table 2

Primary kinetic isotope effects (KIEs) on 2′ nucleophile ($^{18}k_{Nu}$) and 5′ leaving ($^{18}k_{Lg}$) oxygens, and secondary KIEs on O1P ($^{18}k_{O1P}$) and O2P ($^{18}k_{O2P}$) oxygens in aqueous solution for the TS_1 and TS_2 transition states, along with the most relevant available experimental results for comparison.[a]

Reaction	TS_1		TS_2		Expt	
	$18k_{Nu}$	$18/34k_{Lg}$	$18k_{Nu}$	$18/34k_{Lg}$	$18k_{Nu}$	$18/34k_{Lg}$
Native	1.017	1.006	**0.968**	**1.059**	0.981(3)[b]	1.034(4)[b]
S3′	**1.043**[c]	**1.008**[c]	0.992[c]	1.049[c]	1.119(6)[d]	1.0118(3)[d]
S5′	**1.042**[c]	**1.002**[c]	n.a.[e]	n.a.[e]	1.025(5)[d]	1.0009(1)[d]

Reaction	TS_1		TS_2		Expt	
	$18k_{O1P}$	$18k_{O2P}$	$18k_{O1P}$	$18k_{O2P}$	$18k_{O1P}$	$18k_{O2P}$
Native	1.004	1.004	**1.005**	**1.003**	0.999(1)[f]	0.999(1)[f]
S3′	**1.004**[c]	**1.004**[c]	1.002[c]	1.003[c]	n.d.[g]	n.d.[g]
S5′	**1.004**[c]	**1.004**[c]	n.a.[e]	n.a.[e]	n.d.[g]	n.d.[g]

[a] Temperatures used in calculations are identical to those used in the experiments that are being compared: 37°C for native reactions, and 80°C for thio-substituted reactions. All primary KIE values are computed using the second order Kleinert's variational perturbation theory with decoupled instantaneous normal coordinate approximation, while the secondary KIE values are computed using the Bigeleisen equation in the decoupled rigid-rotor harmonic-oscillator approximation.[27, 28] **Boldface** type represents the rate controlling KIE value as determined by comparison with experimental KIE measurements. Experimental errors in the last decimal place are given in parenthesis.

[b] Extracted from Ref. [12] in which the observed $^{18}k_{Nu}$ has been corrected for deprotonation.

[c] To be consistent with the experiments in Ref. [13], the KIE values are calculated with the nucleophile O2′ protonated in the reactant state.

[d] Extracted from Ref. [13], in which the nucleophile O2′ is protonated in the reactant state.

[e] Not applicable as TS_2 cannot be found.

[f] New experimental data given in this work; values represent an average observed for O1P and O2P positions.

[g] Not determined yet by experiments.